# Molecular Mechanism of Apolipoprotein E Binding to Lipoprotein Particles[†]

David Nguyen, Padmaja Dhanasekaran, Michael C. Phillips, and Sissel Lund-Katz*

*Lipid Research Group, Division of Gastroenterology, Hepatology and Nutrition, The Children's Hospital of Philadelphia, University of Pennsylvania School of Medicine, Philadelphia, Pennsylvania 19104-4318*

*Received January 15, 2009; Revised Manuscript Received February 10, 2009*

ABSTRACT: The exchangeability of apolipoprotein (apo) E between lipoprotein particles such as very low-density lipoprotein (VLDL) and high-density lipoprotein (HDL) is critical for lipoprotein metabolism, but despite its importance, the kinetics and mechanism of apoE−lipoprotein interaction are not known. We have used surface plasmon resonance (SPR) to monitor in real time the reversible binding of apoE to human VLDL and $HDL_3$; biotinylated lipoproteins were immobilized on a streptavidin-coated SPR sensor chip, and solutions containing various human apoE molecules at different concentrations were passed across the surface. Analysis of the resultant sensorgrams indicated that the apoE3−lipoprotein interaction is a two-step process. After an initial interaction, the second slower step involves opening of the N-terminal helix bundle domain of the apoE molecule. Destabilization of this domain leads to more rapid interfacial rearrangement which is seen when the lipoprotein binding of apoE4 is compared to that of apoE3. The resultant differences in interfacial packing seem to underlie the differing abilities of apoE4 and apoE3 to bind to VLDL and $HDL_3$. The measured dissociation constants for apoE binding to these lipoprotein particles are in the micromolar range. C-Terminal truncations of apoE to remove the lipid binding region spanning residues 250−299 reduce the level of binding to both types of lipoprotein, but the effect is weaker with $HDL_3$; this suggests that protein−protein interactions are important for apoE binding to this lipoprotein while apoE−lipid interactions are more significant for VLDL binding. The two-step mechanism of lipoprotein binding exhibited by apoE is likely to apply to other members of the exchangeable apolipoprotein family.

There is great interest in understanding the structure−function relationships of apolipoprotein (apo)[1] E because of its pronounced anti-atherogenic properties (*1*). ApoE protects against the development of atherosclerosis, in part, by binding to lipoprotein particles and mediating their clearance from the plasma compartment via interaction with cell surface receptors, notably those of the low-density lipoprotein (LDL) receptor family (*2, 3*). ApoE also promotes the cellular uptake of lipoprotein particles by binding to cell surface heparan sulfate proteoglycans (*4*). The endocytosis of apoE-containing lipoprotein particles reduces plasma cholesterol levels and, thereby, the risk for developing cardiovascular disease (*1*).

Human apoE is a 299-residue single-polypeptide chain that folds into two tertiary structure domains; the N-terminal region (residues 1−191) forms a helix bundle, while the C-terminal region is folded separately into some unknown structure (*3, 5, 6*). ApoE binds readily to lipoprotein particles such as very low-density lipoprotein (VLDL) and high-density lipoprotein (HDL) and forms both exchangeable and nonexchangeable pools (*7, 8*). However, the mechanisms by which apoE associates with and dissociates from lipoprotein particles are not known. Human apoE exhibits polymorphism, and the two common isoforms, apoE3 and apoE4 (which differ by the C112R mutation), partition differently between HDL and VLDL particles (*9*); this effect occurs because of variations in the interactions between the N- and C-terminal domains so that apoE4 binds preferentially to VLDL whereas apoE3 prefers HDL (*6*). This differential lipoprotein binding leads to variations in the lipoprotein profile such that apoE4 is associated with higher plasma cholesterol levels and an increased risk of cardiovascular disease relative to individuals with apoE3 (*10, 11*). The molecular basis for these isoform effects on lipoprotein binding is not well understood.

To address some of the unresolved issues about apoE−lipoprotein interaction, we have used surface plasmon resonance (SPR) to study the reversible binding of apoE to VLDL and HDL particles in real time. SPR has been employed successfully to assess the binding of apoE to proteoglycans (*12*−*15*) and members of the LDL receptor family (*16*) and to assess the binding of enzymes to lipoprotein particles (*17, 18*). These results show that apoE binds by a two-step mechanism to HDL and VLDL.

## EXPERIMENTAL PROCEDURES

*Materials.* $HDL_3$ and VLDL were purified by sequential density ultracentrifugation (*19, 20*) from a pool of fresh human plasma obtained by combining several single units

[†] This research was supported by NIH Grant HL56083.

* To whom correspondence should be addressed: Children's Hospital of Philadelphia, Joseph Stokes Jr. Research Institute, 3615 Civic Center Blvd., Suite 1102 ARC, Philadelphia, PA 19104-4318. Telephone: (215) 590-0588. Fax: (215) 590-0583. E-mail: katzs@email.chop.edu.

[1] Abbreviations: apo, apolipoprotein; $B_{max}$, saturating amount bound; HDL, high-density lipoprotein; $K_d$, dissociation constant; LDLR, low-density lipoprotein receptor; RU, resonance unit; SPR, surface plasmon resonance; VLDL, very low-density lipoprotein; WT, wild type.

10.1021/bi9000694 CCC: $40.75 
Published on Web 02/11/2009

from normolipidemic individuals. Full-length human apoE3, apoE4, and their 22 kDa (residues 1−191), 12 kDa (residues 192−299), and 10 kDa (residues 222−299) fragments were expressed and purified as described previously (*21*−*23*). The C-terminal truncation variants (Δ251−299, Δ261−299, and Δ273−299) of apoE3 and apoE4 were created as described previously (*24, 25*). The apoE preparations were at least 95% pure as assessed by SDS−PAGE. In all experiments, the apoE sample was freshly dialyzed from a 6 M GdnHCl and 1% $\beta$-mercaptoethanol (or 5 mM DTT) solution into a buffer solution before use.

*Biotinylation of HDL and VLDL Particles.* $HDL_3$and VLDL were dialyzed into phosphate-buffered saline (pH 7.4) prior to biotinylation. The EZ-link sulfo-NHS-LC-biotinylation kit from Pierce Chemical Co. (Rockford, IL) was used for attaching biotin molecules through a 2.24 nm spacer arm to lysine residues on the surface of the lipoprotein particles. $HDL_3$ and VLDL, each at 1.0 mg of protein/mL, were mixed with a freshly made 10 mM sulfo-NHS-LC-biotin solution at a 10-fold molar excess of biotin. The lipoproteins were incubated under nitrogen at 4 °C overnight before dialysis against Tris-buffered saline (TBS, pH 7.4) to remove unreacted sulfo-NHS-LC-biotin. The degree of biotinylation of the particles was determined using conditions recommended by Pierce. Briefly, solutions containing biotinylated lipoproteins were added to a mixture of HABA reagent [2-(4′-hydroxyphenyl)-azobenzoic acid] and immunopure avidin (Pierce Chemical Co.). Because of its higher affinity for avidin, biotin, from the biotinylated lipoproteins, displaced avidin-bound HABA. Therefore, the absorbance at 500 nm of the HABA−avidin complex was reduced. The change in absorbance was used to calculate the level of biotin incorporated into the lipoprotein particles. This procedure yielded an average degree of labeling of one biotin molecule per lipoprotein particle.

*Surface Plasmon Resonance (SPR).* Studies of the binding of apolipoproteins (association and dissociation) to $HDL_3$ and VLDL were performed with a Biacore 3000 SPR instrument (Biacore, Uppsala, Sweden) using SA sensor chips (Biacore). This chip is designed to bind biotinylated ligands through a high-affinity capture process. Prior to immobilization of $HDL_3$ or VLDL on the sensor chip, the streptavidin surface was conditioned with three consecutive 1 min injections of 1 M NaCl in 50 mM NaOH (50 $\mu$L/min). The biotinylated $HDL_3$ or VLDL was then immobilized onto the surface through the quasi-covalent biotin−streptavidin interaction by exposing the surface to the biotinylated lipoprotein solutions in running buffer (50 mM TBS, pH 7.4) until 2500−3000 and 5000−7000 response units (RU) of biotinylated $HDL_3$ or VLDL, respectively, were bound to the surface. This was achieved by a 10 $\mu$L injection of biotinylated $HDL_3$ or VLDL (1.0 mg of protein/mL) at a flow rate of 2 $\mu$L/min at room temperature. After 5 min, the chip was washed with degassed TBS to remove unattached lipoprotein. A 50 $\mu$g/mL human apoE3 solution was passed over the chip at a rate of 20 $\mu$L/min for 2 min to block any remaining hydrophobic surface areas and reduce the subsequent level of apoE binding to nonlipoprotein sites; the chip was then washed with TBS until the SPR signal reached a steady background value. The surface of the immobilized $HDL_3$ or VLDL was then exposed to a 4 min injection of apoE dissolved in degassed TBS at a flow rate of 20 $\mu$L/min to monitor association, and then TBS alone was passed over the sensor surface to monitor dissociation of apoE from the immobilized lipoprotein particles. For these experiments, two flow cells were monitored simultaneously with flow cells 1 and 2 containing immobilized biotinylated VLDL and $HDL_3$, respectively. A sensor chip lacking immobilized lipoprotein could not be used as a reference cell because apoE bound more to this surface than to a lipoprotein-coated chip. The apolipoproteins were dialyzed from 6 M GdnHCl containing 5 mM DTT into TBS, filtered (Ultrafree-MC centrifugal filter devices, 0.1 $\mu$m filter unit, Millipore, Bedford, MA), and degassed before serial dilutions (2.5−50 $\mu$g/mL) were made just prior to injection. The sensor chip was washed two times with 20 $\mu$L of TBS between each injection of apolipoprotein. The chips were used for 2 days in repetitive experiments. Regeneration of the sensor chip surface was not possible since the lipoproteins were directly immobilized via biotin−streptavidin interaction. The apoE sensorgrams were independent of flow rate in the range of 10−40 $\mu$L/min, indicating that the apoE binding at 20 $\mu$L/min was not limited by mass transport (diffusion) effects. Steady-state binding isotherms and $K_d$ values of the binding to $HDL_3$ and VLDL were obtained by generating sensorgrams at different apoE concentrations. The sensorgrams were analyzed with the BIA evaluation software, version 4.1 (Biacore). The response curves of various apolipoprotein (analyte) concentrations were fitted to the two-state binding model described by the following equation (*26, 27*).

$$A + B \underset{k_{d1}}{\overset{k_{a1}}{\rightleftarrows}} AB \underset{k_{d2}}{\overset{k_{a2}}{\rightleftarrows}} AB_x \quad (1)$$

The equilibrium constants of each binding step are $K_1 = k_{a1}/k_{d1}$ and $K_2 = k_{a2}/k_{d2}$, and the overall equilibrium binding constant is calculated as $K_a = K_1(1 + K_2)$ and $K_d = 1/K_a$. In this model, the analyte (A) binds to the ligand ($HDL_3$ or VLDL) (B) to form an initial complex (AB) and then undergoes subsequent binding or conformational change to form a more stable complex ($AB_x$). A further check of the two-state binding mechanism was obtained by variation of the contact time for association between apoE and the lipoprotein particle. For a two-state reaction, an increase in the contact time between the analyte and the ligand decreases the dissociation rate since more of the stable $AB_x$ complex is formed. For the apolipoproteins, binding responses in the steady-state region of the sensorgrams ($R_{eq}$) were also plotted against apolipoprotein concentration ($C$) to determine the overall equilibrium binding affinity. The data were subjected to nonlinear regression fitting (Prism 4, GraphPad Inc.) according to the following equation:

$$R_{eq} = CR_{max}/(C + K_d) \quad (2)$$

$R_{max}$ is the maximum binding response, and $K_d$ is the dissociation constant. This SPR approach for measuring $K_d$ is validated by the fact that monitoring the binding of apoE3 and apoE4 to VLDL by ultracentrifugation yielded similar $K_d$ values (*23*).

## RESULTS

*Kinetics and Mechanism of ApoE Binding to VLDL and $HDL_3$.* Figure 1 shows the immobilization of biotinylated $HDL_3$ and VLDL on a streptavidin-coated sensor chip when

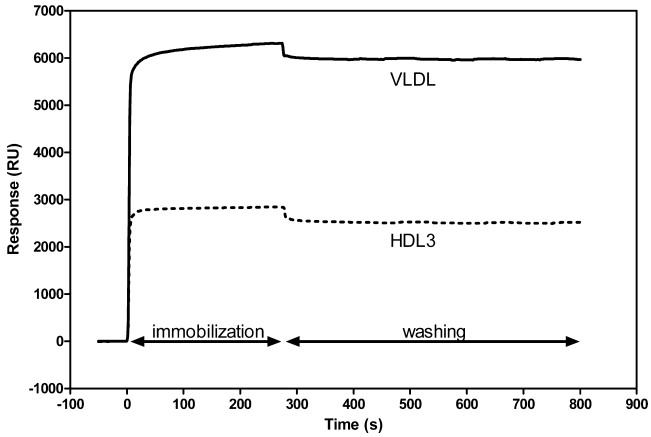


FIGURE 1: Immobilization of VLDL and $HDL_3$ on an SPR sensor chip. Biotinylated VLDL or $HDL_3$ was immobilized on a pretreated streptavidin-coated sensor chip by passing a 1 mg/mL solution across the chip for 5 min at 2 $\mu$L/min and washing with Tris-buffered saline at 100 $\mu$L/min.

a solution of the lipoprotein is passed across the surface. It is apparent that there is rapid binding to give a steady-state level. Flowing buffer solution alone across the chip washes away a small amount of weakly bound lipoprotein, but the remainder is essentially irreversibly bound by the biotin−streptavidin interaction. In multiple experiments, the amounts of $HDL_3$ and VLDL immobilized by this procedure were 2633 ± 508 and 5893 ± 1247 RU (mean ± standard deviation), respectively. It should be noted that these RU levels for bound $HDL_3$ and VLDL cannot be simply interpreted in terms of relative masses of immobilized lipoprotein because of different refractive index properties due to different lipid:protein stoichiometries. The immobilization of $HDL_3$ or VLDL in this fashion permits evaluation of the binding of apoE which is difficult to monitor in solution because of problems, particularly in the case of $HDL_3$, in readily separating the lipoproteins and unbound apoE. Another advantage of the SPR method is that labeling the apoE molecules is not required and the association−dissociation reactions can be monitored in real time. A potential problem in the SPR experiment is steric restriction of apoE binding by the proximity of the sensor chip surface, but because the $HDL_3$ and VLDL particles are attached to the surface by a 2.24 nm spacer arm, protein molecules can access the lipoprotein surface. For example, LCAT (*17*) and CETP (*28*) have been shown to bind to HDL in similar SPR experiments.

The sensorgram obtained when a 50 $\mu$g/mL apoE3 solution was passed across the sensor chip with immobilized VLDL is shown in Figure 2A. The data are corrected for bulk refractive index effects and fitted using a two-state binding model (eq 1). The kinetic data were not fitted well by a 1:1 Langmuir binding model as reflected by larger values of the goodness of fit parameter ($\chi^2$) (data not shown). It follows that the binding of apoE3 to VLDL particles involves either a sequential two-step process or some conformational change (*14, 26, 27*). The binding of apoE3 to $HDL_3$ is also best described by the two-state binding model (data not shown). The deconvoluted curves in Figure 2A show the initial binding (AB) and subsequent binding or conformational changes ($AB_x$). Because of uncertainties about the valences of the lipoprotein particles (the $HDL_3$ and VLDL particles are heterogeneous and do not contain a discrete

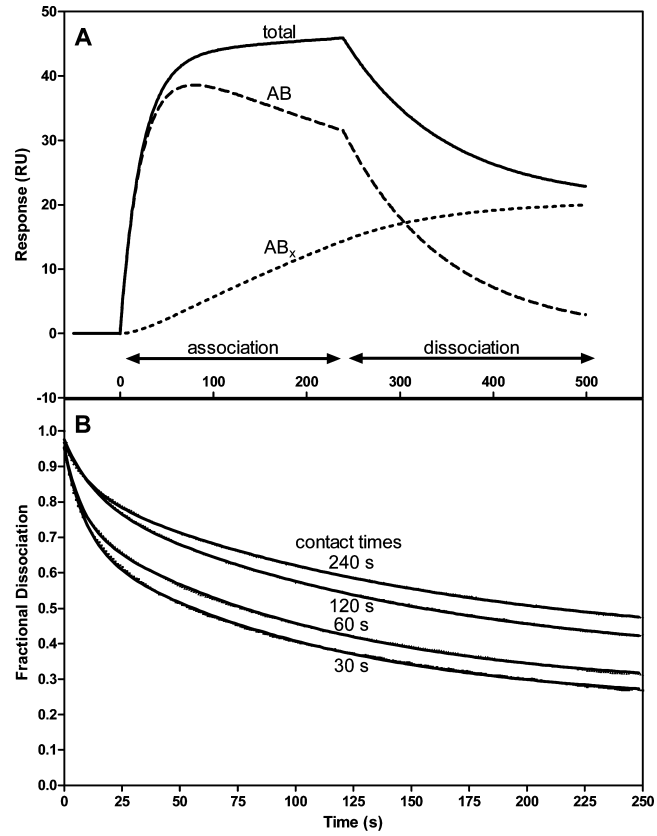


FIGURE 2: Two-state binding of apoE3 to VLDL as detected by SPR measurement of the kinetics of association and dissociation. (A) The sensorgram (—) is for 50 $\mu$g/mL apoE3 at a flow rate of 20 $\mu$L/min. The experimental data were fitted to the two-state binding model where A + B ↔ AB ↔ $AB_x$. The deconvoluted curves are the additive components of the fitted curve and show the initial binding (AB) and the subsequent binding or conformational change ($AB_x$). (B) The dissociation curves show the effect of an increased injection or contact time on the stability of the apoE3−VLDL complex. The experimental dissociation data (---) were fitted to a biexponential decay equation (—).

number of binding sites), it is difficult to interpret the kinetics of association in detail. However, inspection of the deconvoluted curves in Figure 2A reveals that at the end of the 4 min association phase of the experiment, the size of the AB pool of bound apoE3 is approximately twice that of the $AB_x$ pool. It is also apparent that in the dissociation phase (after 4 min), apoE3 molecules in the AB pool dissociate more readily than those in the $AB_x$ pool. By analyzing several sensorgrams, we find the value for the dissociation rate constant $k_{d1}$ for the AB pool is in the range of $2-9 \times 10^{-2}$ $s^{-1}$ while the value of $k_{d2}$ for the $AB_x$ pool is ~50 times smaller. These $k_d$ values correspond to half-times of dissociation of ~14 s and ~10 min for the AB and $AB_x$ pools, respectively. The rate of dissociation of apoE3 from the VLDL surface is dependent upon the length of time the apoE3 is in contact with the particle. As shown in Figure 2B, progressively shortening the injection (contact) time from 240 s to 60 and 30 s enhances dissociation of apoE3 from the VLDL surface. The fitting data indicate that the fraction of apoE3 in the AB pool approximately doubles to 0.25 as the contact time is decreased to 30 s. The value of $k_{d1}$ for the AB pool is not affected by the change in contact time, whereas $k_{d2}$ increases by ~40% as the contact time is decreased to 30 s. These results are consistent with the second

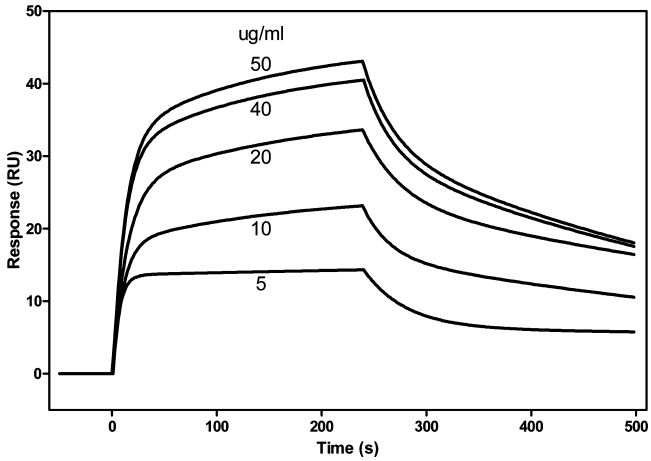


FIGURE 3: Representative SPR sensorgrams of binding of human apoE to immobilized lipoprotein. ApoE solutions at the indicated concentrations were passed across the sensor chip, and the experimental data were fitted with the two-state binding model, where A + B ↔ AB ↔ $AB_x$ (see Experimental Procedures).

step in the two-step mechanism of apoE3 binding to VLDL involving a conformational change in the bound apoE molecules.

*Influence of ApoE Domain Structure on Lipoprotein Binding*. Figure 3 shows a typical series of sensorgrams for binding of apoE at different concentrations to immobilized lipoprotein. Fitting of sensorgrams of this type with the two-state binding model yields a maximal binding value ($R_{max}$) for each concentration of apoE3. Figure 4A shows a steady-state binding isotherm for WT apoE3 binding to VLDL plotted using such $R_{max}$ values and fitted to a one-site binding model (eq 2). The data in Figure 4A yield a $K_d$ value of 20 ± 5 μg of apoE3/mL (0.6 ± 0.1 μM, mean ± standard error of the mean) for the binding of human apoE3 to $VLDL_3$. This $K_d$ value indicates that the apoE3−VLDL interaction is of moderate affinity and is in agreement with the value of 23 ± 4 μg/mL reported previously by us using an ultracentrifuge method (*23*). Figure 4A compares the isotherms obtained for WT human apoE3 and its separate N-terminal (residues 1−191) and C-terminal (residues 192−299 and 222−299) domains binding to VLDL; the $K_d$ and $B_{max}$ values derived from these isotherms are listed in Table 1. It is apparent that removal of the C-terminal domain to form 22 kDa apoE3 gives rise to a weakly hyperbolic binding isotherm so that the errors in the $K_d$ and $B_{max}$ determinations are large (Table 1). Neither the amount of apoE3 that binds ($B_{max}$) nor the binding affinity ($K_d$) is altered significantly by removal of the C-terminal domain, although there is a trend toward a higher $K_d$ value for 22 kDa apoE3, especially when considered on a molar basis (Table 1). In contrast, the isolated apoE 10 and 12 kDa C-terminal fragments exhibit clearly saturable binding to VLDL (Figure 4A); the $K_d$ values are lower than that for WT apoE3 (Table 1), indicating higher binding affinity. Interestingly, the presence of the so-called hinge region (residues 192−221) (*3*) in 12 kDa apoE does not change the binding from that found with the isolated C-terminal 10 kDa apoE domain. Inspection of Figure 4B and the $K_d$ and $B_{max}$ values listed in Table 1 indicate that the pattern of lipoprotein binding of the apoE3 domains is similar with VLDL and $HDL_3$.

The tertiary structure domains in the apoE molecule are influenced by polymorphism. ApoE3 is the most prevalent isoform and has normal functionality, whereas the C112R mutation to yield apoE4 induces abnormal behavior (*2*).

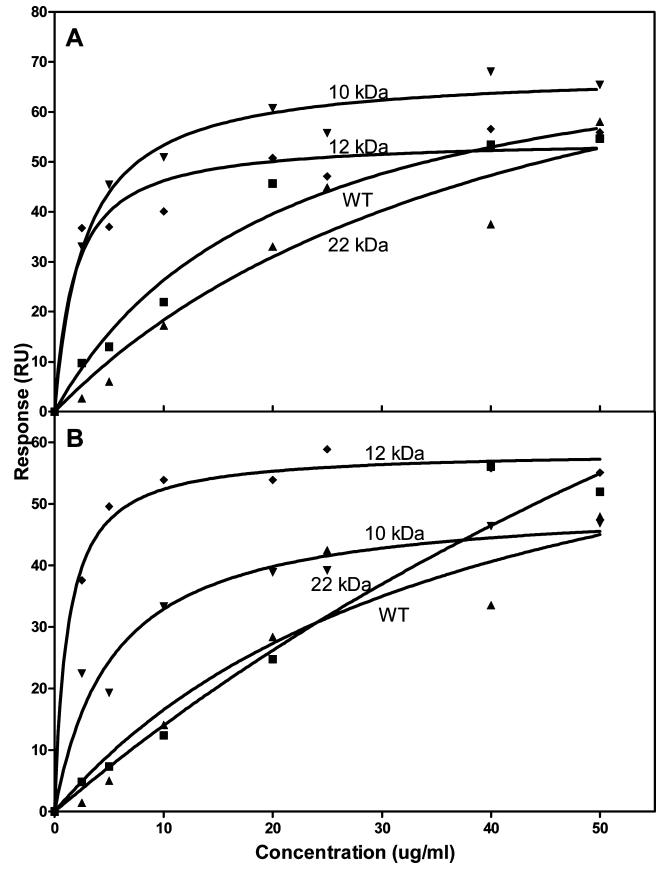


FIGURE 4: Isotherms describing the binding of human apoE3 and its tertiary structure domains to VLDL (A) and $HDL_3$ (B). The maximal response ($RU_{max}$) was derived by fitting sensorgrams obtained over a range of apoE3 concentrations (cf. Figure 3) to the two-state binding model. These $R_{max}$ values are plotted as a function of apoE3 concentration and fitted to a one-site binding model: (■) WT apoE3, (▲) 22 kDa N-terminal domain (residues 1−191), (◆) 12 kDa C-terminal domain (residues 192−299), and (▼) 10 kDa C-terminal domain (residues 222−299).

Table 1: Binding Constants for Interaction of ApoE with VLDL and $HDL_3$

| | $K_d$[a] | | $B_{max}$[b] | |
|---|---|---|---|---|
| apoE | μg/mL | μM | RU | relative |
| | | VLDL | | |
| WT apoE3 | 20 ± 5 | 0.6 ± 0.1 | 80 ± 9 | 1 |
| WT apoE4 | 29 ± 10 | 0.9 ± 0.3 | 173 ± 27[d] | 2.2 |
| 22 kDa apoE3 | 44 ± 39 | 2.0 ± 1.8 | 100 ± 49 | 1.2 |
| 22 kDa apoE4 | 34 ± 12 | 1.5 ± 0.5 | 67 ± 12 | 0.8 |
| 12 kDa apoE | 2.0 ± 0.6[c] | 0.2 ± 0.05 | 55 ± 3[d] | 0.7 |
| 10 kDa apoE | 3.0 ± 0.5[c] | 0.3 ± 0.05 | 68 ± 2 | 0.8 |
| | | $HDL_3$ | | |
| WT apoE3 | 136 ± 100 | 4 ± 3 | 204 ± 116 | 1 |
| WT apoE4 | 31 ± 11 | 0.9 ± 0.3 | 111 ± 19 | 0.5 |
| 22 kDa apoE3 | 38 ± 28 | 1.7 ± 1.3 | 79 ± 31 | 0.4 |
| 22 kDa apoE4 | 47 ± 10 | 2.1 ± 0.5 | 115 ± 14 | 0.6 |
| 12 kDa apoE | 1.2 ± 0.2[c] | 0.1 ± 0.02 | 59 ± 1 | 0.3 |
| 10 kDa apoE | 5.3 ± 1.4[c] | 0.5 ± 0.1 | 50 ± 3 | 0.2 |

[a] The $K_d$ and $B_{max}$ values are listed as means ± the standard error of the mean and are derived from representative binding isotherms of the type shown in Figure 4. [b] The $B_{max}$ values for the VLDL and $HDL_3$ binding experiments cannot be compared directly because different amounts of lipoprotein are immobilized on the SPR chip. [c] Significantly different ($p < 0.05$) from the $K_d$ for WT apoE3. [d] Significantly different from the $B_{max}$ for WT apoE3.

Introduction of the arginine residue at position 112 destabilizes the N-terminal helix bundle domain (*29, 30*) and alters the interaction between the N- and C-terminal domains (*3, 6*). The altered domain−domain interactions are known to underlie the differing preferences of apoE3 and apoE4 for binding to HDL and VLDL (*9, 23, 25, 31, 32*). To examine what effect, if any, the apoE3/apoE4 polymorphism has on the mechanism and kinetics of lipoprotein interaction, the binding of these isoforms to VLDL and $HDL_3$ was compared by SPR. Isotherms of the type shown in Figure 4 were generated, and the resultant $K_d$ and $B_{max}$ values are listed in Table 1. In the case of VLDL, the $K_d$ values are the same, indicating that the binding affinity for apoE3 is essentially unaltered by the C112R mutation. However, the $B_{max}$ for apoE4 is approximately twice that for apoE3, consistent with prior observations that apoE4 partitions more to VLDL when added to plasma (*9*). In the case of $HDL_3$, the situation is reversed with the $B_{max}$ for apoE3 being the highest (Table 1). As mentioned earlier, the apoE3−$HDL_3$ binding isotherm is quasi-linear which leads to large uncertainties in the derived $K_d$ values, and because of this, a significant difference in binding affinity could not be detected. Similar considerations apply to the binding data for 22 kDa apoE3 and 22 kDa apoE4 because the binding to both VLDL and $HDL_3$ was not readily saturable and the binding isotherms were quasi-linear. However, it is apparent from the $B_{max}$ values in Table 1 that the isolated 22 kDa N-terminal domains of apoE3 and apoE4 do not discriminate between $HDL_3$ and VLDL like the intact apoE3 and apoE4 molecules do.

The sensorgram in Figure 2A shows that when apoE3 binds to VLDL the kinetics of binding are such that at the end of the association phase (240 s), the AB pool is larger than the $AB_x$ pool. The sensorgram and deconvolution curves in Figure 5A demonstrate that the kinetics are different for apoE4 binding to VLDL; in this case, the $AB_x$ pool is larger than the AB pool at 240 s. This more rapid shift to the $AB_x$ pool for apoE4 compared to apoE3 is associated with higher values for the rate constants, $k_{d1}$ and $k_{a2}$ (eq 1). Similar differences in kinetics are seen when apoE3 and apoE4 bind to $HDL_3$ (data not shown). The data in Figure 5B demonstrating that the AB and $AB_x$ pools for 22 kDa apoE4 binding to VLDL at 240 s are similar in size indicate that the presence of both structural domains is required for the relatively rapid transition to the $AB_x$ state seen with apoE4. Consistent with the concept, the $AB_x$ pool observed when 12 kDa apoE binds to VLDL is smaller than the AB pool at 240 s (Figure 5C). The 10 kDa apoE C-terminal domain exhibits similar behavior (data not shown).

*Influence of C-Terminal Residues on ApoE Binding to VLDL and $HDL_3$.* The data in Figure 4 and Table 1 showing that the C-terminal 10 and 12 kDa domains are capable of higher-affinity, saturable, binding to VLDL and $HDL_3$ are consistent with prior reports (*3, 31, 33*) of the importance of the region spanning residues 250−299 for lipid binding. To further explore the contributions of this part of the apoE molecule to binding to VLDL and $HDL_3$, we employed apoE3 and apoE4 variants with residues 273−299, 261−299, and 251−299 deleted. The physical properties of these engineered apoE3 and apoE4 molecules have been characterized previously (*24, 25*). The isotherms in Figure 6A show that C-terminal truncation reduces the level of apoE4 binding to VLDL; in particular, the $B_{max}$ values for the 1−260 and

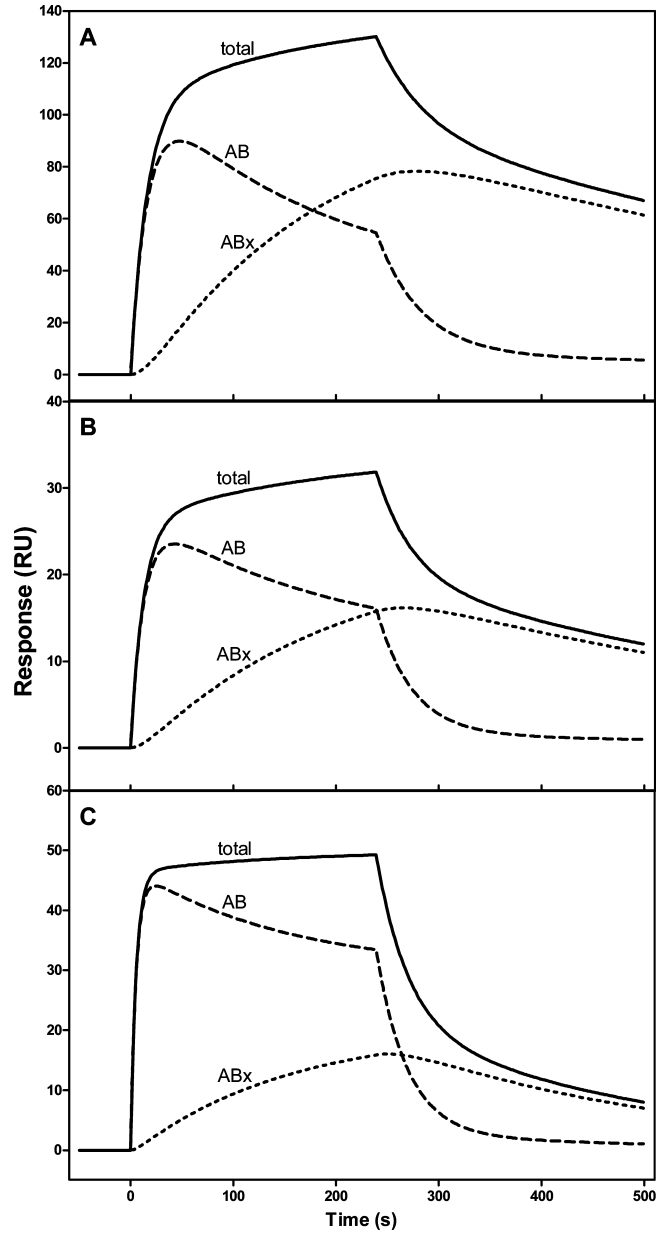


FIGURE 5: SPR sensorgrams of binding of WT human apoE4 (A) and its N-terminal (residues 1−191) (B) and C-terminal (residues 192−299) (C) tertiary structure domains to immobilized VLDL. The sensorgrams for total binding (—) are for 50 $\mu$g/mL apoE4 or fragment at a flow rate of 20 $\mu$L/min, and the initial binding (AB) and subsequent binding ($AB_x$) contributions were obtained by deconvolution, as described in the legend of Figure 2.

1−250 variants are significantly reduced. The results also show that removing residues 273−299 has a relatively small effect and that residues 261−272 make a marked contribution to binding (cf. refs *24* and *31*). These C-terminal truncations in apoE3 have similar effects on VLDL binding (Figure 6B); the hyperbolic nature of the binding isotherms is reduced for the C-terminal truncation variants, and saturation is not evident in the concentration range covered. The data in Figure 6C,D show that the C-terminal truncations cause smaller reductions in the levels of binding of apoE3 and apoE4 to $HDL_3$ compared to the situation with VLDL (Figure 6A,B). Since residues in the 250−299 region promote lipid interactions, their small contribution to the binding of apoE3 and apoE4 to $HDL_3$ implies that protein−lipid interactions are not a major factor in this case.

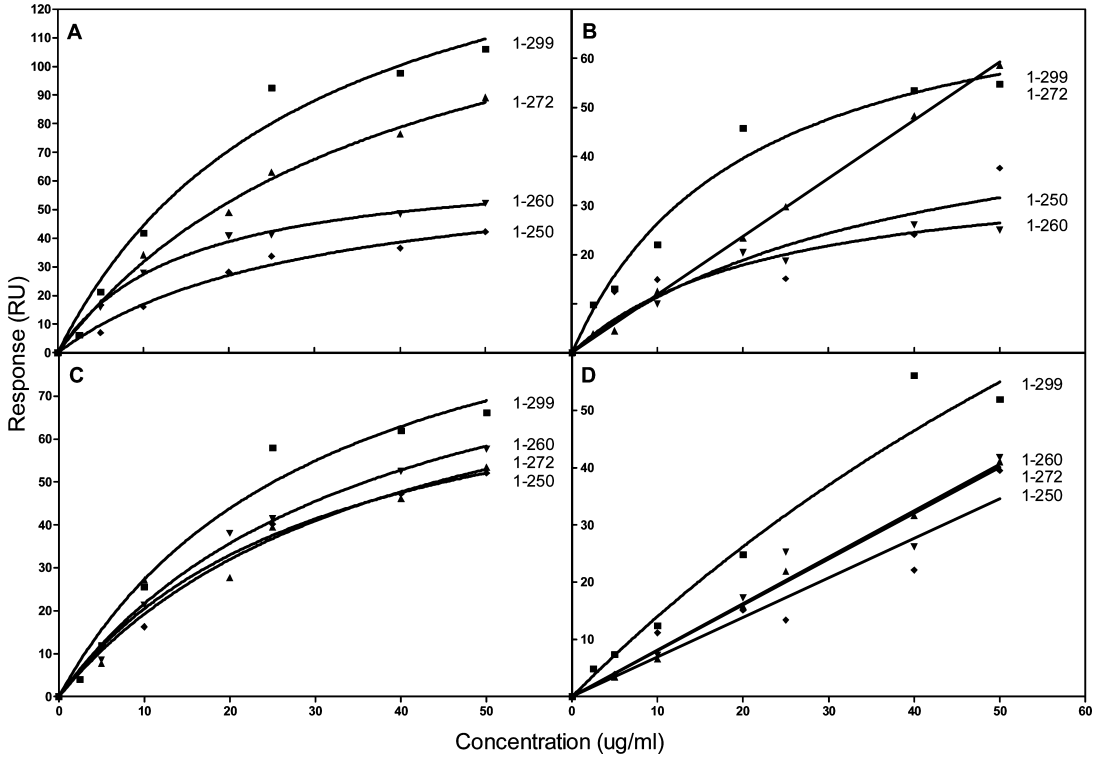


FIGURE 6: Influence of C-terminal truncation on the binding of apoE3 and apoE4 to VLDL and $HDL_3$: (A) apoE4 binding to VLDL, (B) apoE3 binding to VLDL, (C) apoE4 binding to $HDL_3$, and (D) apoE3 binding to $HDL_3$. The binding isotherms were obtained and analyzed as described in the legend of Figure 4: (■) WT apoE, (▲) apoE variant (1−272), (▼) apoE variant (1−260), and (◆) apoE variant (1−250).

## DISCUSSION

This SPR study gives the first direct measurements of real-time association of apolipoprotein with and dissociation of apolipoprotein from lipoprotein particles. The fact that the sensorgrams for the interaction of apoE with VLDL and $HDL_3$ are best fitted to a two-state model indicates that some sequential binding or conformational events occur. Given that apoE can exist in two lipid-bound states on spherical lipid particles (*22, 34*) with the N-terminal four-helix bundle in either open or closed conformations (*3, 35, 36*), it is likely that this conformational change underlies the two-step kinetics seen when apoE binds to VLDL or $HDL_3$. A model incorporating this concept is presented in Figure 7. On this basis, the second $AB_x$ phase of binding for apoE3 or apoE4 corresponds, at least in part, to the rate of helix bundle unfolding. The fact that the isolated 12 kDa C-terminal domain of apoE also exhibits a small $AB_x$ phase (Figure 5C) indicates that other conformational changes besides helix bundle opening occur when apoE binds to VLDL or $HDL_3$. Also, the C-terminal domain is not essential for initiating binding of apoE to a lipoprotein particle because the 22 kDa N-terminal fragments of apoE3 and apoE4 can bind to some extent (Table 1).

The isotherms depicted in Figure 4 together with the binding constants listed in Table 1 show clearly that the isolated 10 and 12 kDa apoE C-terminal domains can bind in a saturable, high-affinity, fashion to VLDL and $HDL_3$. Consistent with the extreme C-terminal part of the apoE molecule being important for lipid binding, deletion of residues in the 250−299 region reduces the extent of lipoprotein association (*24, 25, 31, 33, 37*). The finding (Figure 6) that such truncations cause larger reductions in

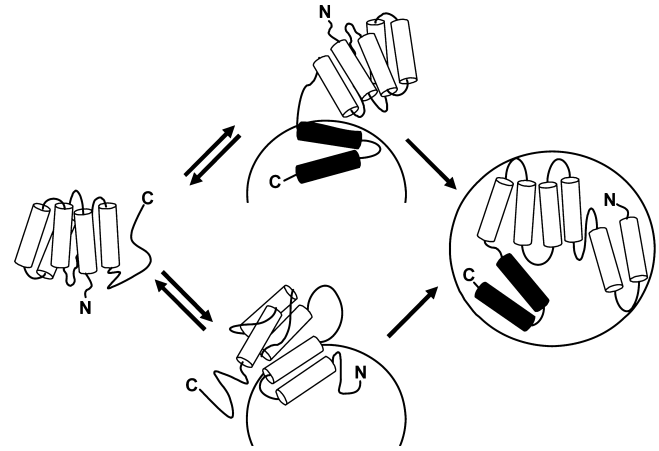


FIGURE 7: Model of the two-step mechanism of binding of apoE to a spherical VLDL or $HDL_3$ particle. Initial binding (step 1) is rapid and readily reversible and occurs through amphipathic α-helices in either the C-terminal domain or the N-terminal helix bundle domain. Step 2 involves the subsequent opening of the helix bundle whereby hydrophobic helix−helix interactions are converted to helix−lipid interactions. Step 2 is relatively slow and less readily reversible.

binding of apoE3 and apoE4 to VLDL than to $HDL_3$ implies that lipid interactions play a bigger role in the former case. This effect might be expected because, compared to $HDL_3$, a larger fraction of the VLDL particle surface contains exposed phospholipid molecules. In the case of $HDL_3$, a large fraction of the particle surface is covered by the resident apolipoproteins so that apoE binding is more likely to involve protein−protein interactions.

Prior comparisons of apoE3 and apoE4 have attributed the differences in preference for binding to $HDL_3$ and VLDL to differences in binding affinity rather than binding

capacity (*22, 23, 32*). The relatively low affinity and the lack of saturability of binding of apoE3 and apoE4 to VLDL and $HDL_3$ indicated by the current SPR experiments make detection of differences in binding affinity difficult. However, the binding parameters in Table 1 suggest that the variations in binding of the apoE isoform to VLDL and $HDL_3$ are, at least in part, a consequence of differences in the ability to be accommodated on the lipoprotein particle surface. Since the second $AB_x$ phase for apoE4 binding to VLDL is greater than that for apoE3 (cf. Figures 2A and 5A), it follows from the model in Figure 7 that the helix bundle in apoE4 opens more readily. This effect might be expected because the N-terminal domain of apoE4 is less stable than that of apoE3 (*29, 30*). On this basis, apoE4 would require more interfacial area than apoE3 (where the helix bundle would be more likely to remain closed and out of contact with the surface; see step 1 in Figure 7) and consequently favor binding to the larger VLDL particle. The smaller $HDL_3$ particle would more readily accommodate apoE3 molecules with only the C-terminal domain occupying interfacial area.

The fact that apoE binding to lipoprotein particles involves a two-step mechanism has physiological implications in that it explains the existence of exchangeable and nonexchangeable pools of apoE on the surface of lipoprotein particles. Thus, apoE molecules that are absorbed with the helix bundle domain closed (step 1 in Figure 7) can exchange readily, whereas those apoE molecules absorbed with the helix bundle open (step 2) do not exchange easily. Since the low-density lipoprotein receptor (LDLR) binding site in apoE is not recognized when the helix bundle is closed but only when it is open (*3*), it is expected that only molecules that achieve step 2 binding will act as effective ligands for the LDLR. This idea explains the fact that apoE in VLDL particles exists in two different conformations, one accessible and one inaccessible to the LDLR (*38*). Thus, apoE molecules bound with the helix bundle open are critical for apoE to achieve its major function of mediating the clearance of remnant lipoprotein particles from the circulation. Since apoE4 binds more than apoE3 to VLDL (Table 1) and it tends to bind in the helix bundle open conformation because the helix bundle is relatively unstable, it is expected that apoE4−VLDL will bind better than apoE3−VLDL to the LDLR. This difference in LDLR binding ability has been observed experimentally (*39*).

In summary, the application of SPR has provided new insights into the mechanism of apoE−lipoprotein interaction and into the contributions of the apoE tertiary structure domains to binding. ApoE binds to VLDL and $HDL_3$ particles by a two-step mechanism with the rate being influenced by the stability and ease of unfolding of the N-terminal helix bundle domain. The mechanism and kinetics of lipoprotein interaction described here for apoE are likely to be relevant to the binding of other exchangeable apolipoproteins that have two-domain tertiary structures.

## REFERENCES


1. Curtiss, L. K., and Boisvert, W. A. (2000) Apolipoprotein E and atherosclerosis. *Curr. Opin. Lipidol. 11*, 243–251.
2. Mahley, R. W., and Rall, S. C. J. (2000) Apolipoprotein E: Far more than a lipid transport protein. *Annu. Rev. Genomics Hum. Genet. 1*, 507–537.
3. Weisgraber, K. H. (1994) Apolipoprotein E: Structure-function relationships. *Adv. Protein Chem. 45*, 249–302.
4. Mahley, R. W., and Ji, S. Z. (1999) Remnant lipoprotein metabolism: Key pathways involving cell-surface heparan sulfate proteoglycans and apolipoprotein E. *J. Lipid Res. 40*, 1–16.
5. Saito, H., Lund-Katz, S., and Phillips, M. C. (2004) Contributions of domain structure and lipid interaction to the functionality of exchangeable human apolipoproteins. *Prog. Lipid Res. 43*, 350–380.
6. Hatters, D. M., Peters-Libeu, C. A., and Weisgraber, K. H. (2006) Apolipoprotein E structure: Insights into function. *Trends Biochem. Sci. 31*, 445–454.
7. van't Hooft, F., and Havel, R. J. (1981) Metabolism of chromatographically separated rat serum lipoproteins specifically labeled with $^{125}$I-apolipoprotein E. *J. Biol. Chem. 256*, 3963–3968.
8. Rubenstein, A., Gibson, J. C., Ginsberg, H. N., and Brown, W. V. (1986) In vitro metabolism of apolipoprotein E. *Biochim. Biophys. Acta 879*, 355–361.
9. Weisgraber, K. H. (1990) Apolipoprotein E distribution among human plasma lipoproteins: Role of the cysteine-arginine interchange at residue 112. *J. Lipid Res. 31*, 1503–1511.
10. Davignon, J., Gregg, R. E., and Sing, C. F. (1988) Apolipoprotein E polymorphism and atherosclerosis. *Arteriosclerosis 8*, 1–21.
11. Lahoz, C., Schaefer, E. J., Cupples, L. A., Wilson, P. W., Levy, D., Osgood, D., Parpos, S., Pedro-Botet, J., Daly, J. A., and Ordovas, J. M. (2001) Apolipoprotein E genotype and cardiovascular disease in the Framingham Heart Study. *Atherosclerosis 154*, 529–537.
12. Shuvaev, V. V., Laffont, I., and Siest, G. (1999) Kinetics of apolipoprotein E isoforms binding to the major glycosaminoglycans of the extracellular matrix. *FEBS Lett. 459*, 353–357.
13. Libeu, C. P., Lund-Katz, S., Phillips, M. C., Wehrli, S., Hernaiz, M. J., Capila, I., Linhardt, R. J., Raffai, R. L., Newhouse, Y. M., Zhou, F., and Weisgraber, K. H. (2001) New insights into the heparin sulfate proteoglycan-binding activity in apolipoprotein E. *J. Biol. Chem. 276*, 39138–39144.
14. Futamura, M., Dhanasekaran, P., Handa, T., Phillips, M. C., Lund-Katz, S., and Saito, H. (2005) Two-step mechanism of binding of apolipoprotein E to heparin. *J. Biol. Chem. 280*, 5414–5422.
15. Yamauchi, Y., Deguchi, N., Takagi, C., Tanaka, M., Dhanasekaran, P., Nakano, M., Handa, T., Phillips, M. C., Lund-Katz, S., and Saito, H. (2008) Role of the N- and C-terminal domains in binding of apolipoprotein E isoforms to heparan sulfate and dermatan sulfate: A surface plasmon resonance study. *Biochemistry 47*, 6702–6710.
16. Ruis, J., Kouiavskaia, D., Migliorini, M., Robinson, S., Saenko, E. L., Gorlatova, N., Li, D., Lawrence, D., Hyman, B. T., Weisgraber, K. H., and Strickland, D. K. (2005) Characterization of the apoE isoform binding properties of the VLDL receptor reveal marked differences from LRP and the LDL receptor. *J. Lipid Res. 46*, 1721–1731.
17. Jin, L., Shieh, J. J., Grabbe, E., Adimoolam, S., Durbin, D., and Jonas, A. (1999) Surface plasmon resonance biosensor studies of human wild-type and mutant lecithin cholesterol acyltransferase interactions with lipoproteins. *Biochemistry 38*, 15659–15665.
18. Gaidukov, L., and Tawfik, D. S. (2005) High affinity, stability, and lactonase activity of serum paraxonase PON1 anchored on HDL with apoA-I. *Biochemistry 44*, 11843–11854.
19. Havel, R. J., Eder, H. A., and Bragdon, J. H. (1955) The distribution and chemical composition of untracentrifugally separated lipoproteins in human serum. *J. Clin. Invest. 34*, 1345–1353.
20. Hatch, F. T., and Lees, R. S. (1968) Practical methods for plasma lipoprotein analysis. *Adv. Lipid Res. 6*, 1–68.
21. Morrow, J. A., Arnold, K. S., and Weisgraber, K. H. (1999) Functional characterization of apolipoprotein E isoforms overexpressed in *Escherichia coli*. *Protein Expression Purif. 16*, 224–230.
22. Saito, H., Dhanasekaran, P., Baldwin, F., Weisgraber, K., Lund-Katz, S., and Phillips, M. C. (2001) Lipid binding-induced conformational change in human apolipoprotein E. *J. Biol. Chem. 276*, 40949–40954.
23. Saito, H., Dhanasekaran, P., Baldwin, F., Weisgraber, K. H., Phillips, M. C., and Lund-Katz, S. (2003) Effects of polymorphism on the lipid interaction of human apolipoprotein E. *J. Biol. Chem. 278*, 40723–40729.
24. Tanaka, M., Vedhachalam, C., Sakamoto, T., Dhanasekaran, P., Phillips, M. C., Lund-Katz, S., and Saito, H. (2006) Effect of carboxyl-terminal truncation on structure and lipid interaction of human apolipoprotein E4. *Biochemistry 45*, 4240–4247.
25. Sakamoto, T., Tanaka, M., Vedhachalam, C., Nickel, M., Nguyen, D., Dhanasekaran, P., Phillips, M. C., Lund-Katz, S., and Saito,

H. (2008) Contributions of the carboxyl-terminal helical segment to the self-association and lipoprotein preferences of human apolipoprotein E3 and E4 isoforms. *Biochemistry 47*, 2968–2977.
26. Karlsson, R., and Falt, A. (1997) Experimental design for kinetic analysis of protein-protein interactions with surface plasmon resonance biosensors. *J. Immunol. Methods 200*, 121–133.
27. Lipschultz, C. A., Li, Y., and Smith-Gill, S. (2000) Experimental design for analysis of complex kinetics using surface plasmon resonance. *Methods 20*, 310–318.
28. Clark, R. W., Ruggeri, R. B., Cunningham, D., and Bamberger, M. J. (2006) Description of the torcetrapib series of cholesteryl ester transfer protein inhibitors, including mechanism of action. *J. Lipid Res. 47*, 537–552.
29. Morrow, J. A., Segall, M. L., Lund-Katz, S., Phillips, M. C., Knapp, M., Rupp, B., and Weisgraber, K. H. (2000) Differences in stability among the human apolipoprotein E isoforms determined by the amino-terminal domain. *Biochemistry 39*, 11657–11666.
30. Acharya, P., Segall, M. L., Zaiou, M., Morrow, J. A., Weisgraber, K., Phillips, M. C., Lund-Katz, S., and Snow, J. W. (2002) Comparison of the stabilities and unfolding pathways of human apolipoprotein E isoforms by differential scanning calorimetry and circular dichroism. *Biochim. Biophys. Acta 1584*, 9–19.
31. Dong, L. M., Wilson, C., Wardell, M. R., Simmons, T., Mahley, R. W., Weisgraber, K. H., and Agard, D. A. (1994) Human apolipoprotein E. Role of arginine 61 in mediating the lipoprotein preferences of the E3 and E4 isoforms. *J. Biol. Chem. 269*, 22358–22365.
32. Dong, L. M., and Weisgraber, K. H. (1996) Human apolipoprotein E4 domain interaction. Arginine 61 and glutamic acid 255 interact to direct the preference for very low density lipoproteins. *J. Biol. Chem. 271*, 19053–19057.
33. Westerlund, J. A., and Weisgraber, K. H. (1993) Discrete carboxyl-terminal segments of apolipoprotein E mediate lipoprotein association and protein oligomerization. *J. Biol. Chem. 268*, 15745–15750.
34. Narayanaswami, V., and Ryan, R. O. (2000) Molecular basis of exchangeable apolipoprotein function. *Biochim. Biophys. Acta 1483*, 15–36.
35. Fisher, C. A., and Ryan, R. O. (1999) Lipid binding-induced conformational changes in the N-terminal domain of human apolipoprotein E. *J. Lipid Res. 40*, 93–99.
36. Narayanaswami, V., Szeto, S. S., and Ryan, R. O. (2001) Lipid association-induced N- and C-terminal domain reorganization in human apolipoprotein E3. *J. Biol. Chem. 276*, 37853–37860.
37. Li, X., Kypreos, K. E., Zanni, E. E., and Zannis, V. (2003) Domains of apoE required for binding to apoE receptor 2 and to phospholipids: Implications for the functions of apoE in the brain. *Biochemistry 42*, 10406–10417.
38. Bradley, W. A., Hwang, S. L., Karlin, J. B., Lin, A. H., Prasad, S. C., Gotto, A. M., Jr., and Gianturco, S. H. (1984) Low-density lipoprotein receptor binding determinants switch from apolipoprotein E to apolipoprotein B during conversion of hypertriglyceridemic very-low-density lipoprotein to low-density lipoproteins. *J. Biol. Chem. 259*, 14728–14735.
39. Knouff, C., Hinsdale, M. E., Mezdour, H., Altenburg, M. K., Watanabe, M., Quarfordt, S. H., Sullivan, P. M., and Maeda, N. (1999) Apo E structure determines VLDL clearance and atherosclerosis risk in mice. *J. Clin. Invest. 103*, 1579–1586.

BI9000694